

PAPER REF: 7158

## **FLUID-STRUCTURE INTERACTION FOR HEMODYNAMIC STUDY IN PATIENT CORONARY ARTERIES - VALIDATION**

**N. Pinho<sup>1</sup>, C.F. Castro<sup>1</sup>, C.C. António<sup>1</sup>, N. Bettencourt<sup>2</sup>, L.C. Sousa<sup>1</sup>, S.I.S. Pinto<sup>1(\*)</sup>**

<sup>1</sup>Inst. Science and Innovation in Mech. and Industrial Engineering (INEGI), FEUP/U.Porto, Portugal

<sup>2</sup>Cardiovascular R&D Unit, Faculty of Medicine, University of Porto, Porto, Portugal

(\*)*Email*: spinto@fe.up.pt

### **ABSTRACT**

This work compares the coronary artery hemodynamics, considering rigid and deformable arterial wall throughout a cardiac cycle. A patient-specific study was performed using computational fluid dynamics (CFD) and fluid-structure interaction (FSI) method. The simulations were run through an In-House OpenFOAM software and the commercial ANSYS® software for validation. The velocity magnitude, at systolic peak, was achieved in several locations, considering CFD and FSI. The major difference was verified in the bifurcation. The dynamic behavior results in a global reduction of 3.5% due to the increase of the fluid domain.

**Keywords:** fluid-structure interaction, hemodynamics, coronary artery, computed tomography.

### **INTRODUCTION**

Cardiovascular diseases have been one of the leading cause of mortality in humans in the worldwide (Mozaffarian *et al.* 2015). From clinical practice, specific sites in the circulatory system are sensitive to the development of atherosclerosis - accumulation of lipoproteins and other fat substances inside the artery and near the wall. This disease blocks the normal circulation of blood flow. The computed tomography (CT) images of coronary arteries provide information about the geometry and the location of the disease. However, the CT scans do not explain the hemodynamics. In this way, numerical studies of blood flow have gained importance and can contribute, as an auxiliary tool, for the prevention and treatment of such diseases.

The left coronary artery (LCA) is a complex artery with many curvatures, bifurcations and roughness. As far as we know, patient-specific studies of the LCA hemodynamics is few explored with conditions as close as possible to the reality. Many studies considered rigid wall of the arteries as simplification (van der Giessen *et al.* 2011, Chaichana *et al.* 2013, Xie *et al.* 2014). The goal of the present work is to validate and conclude about the differences in the hemodynamics considering two different modeling, rigid wall and deformable vessel wall, the last one using a fluid-structure interaction method (FSI).

### **3D GEOMETRY AND MESH RECONSTRUCTION**

The CT images sequence of a LCA case were analysed through the image processing software for 3D design - MIMICS®. From the axial view image sequence of the heart (Figure 1a) the

aorta, the left main stem (LMS), left anterior descending artery (LAD), and the left circumflex artery (LCx) were selected and segmented (Figure 1b). Then, the software automatically obtained the 3D mask and the centreline for the LMS and branches (Figure 1c). The high roughness arising from the segmentation process was reduced using the Materialise 3-Matic® software. The solid domain, defining the artery wall, was obtained by extruding outwards the fluid domain (Figure 1d) and selecting a constant wall thickness equal to 0.5 mm (Guerciotti *et al.* 2017). Both domains were discretized with tetrahedral elements (Figure 1e) using Meshing ANSYS® software. Several mesh tests were performed in order to achieve accurate simulations.

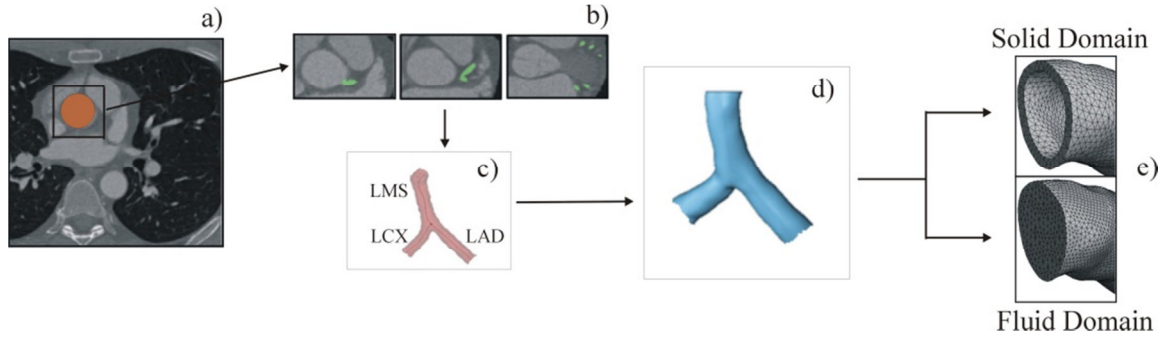


Fig. 1 - a) axial view of the heart - aorta, b) segmentation of the LMS, LAD and LCx, c) 3D mask and centerline of the LMS and branches, d) 3D geometry with the arterial wall, e) tetrahedral mesh of solid and fluid domains.

## BLOOD AND ARTERIAL WALL PROPERTIES

Blood was considered an isotropic, incompressible and homogeneous fluid with constant density,  $\rho_f$ , equal to  $1060 \text{ kg/m}^3$  (Pinto *et al.* 2018). The shear-thinning blood behavior, non-Newtonian fluid, was modulated through Carreau model which properties are well defined in the literature at homeostatic temperature,  $37^\circ\text{C}$  (Pinto *et al.* 2018, Zhang *et al.* 2016):

$$\mu = \mu_\infty + (\mu_0 - \mu_\infty)[1 + (\lambda\dot{\gamma})^2]^{(n-1)/2} \quad (1)$$

$\mu$  is the blood viscosity,  $\mu_\infty$  the infinite shear viscosity ( $0.00345 \text{ Pa}\cdot\text{s}$ ),  $\mu_0$  the zero shear viscosity ( $0.0560 \text{ Pa}\cdot\text{s}$ ),  $\lambda$  the relaxation time ( $3.313 \text{ s}$ ),  $\dot{\gamma}$  the shear rate ( $\text{s}^{-1}$ ), and  $n$  a characteristic constant of the flow ( $0.3568$ ).

The arterial wall was considered as an isotropic, homogeneous, incompressible and non-linear material through the 5-parameter Mooney-Rivlin hyperelastic constitutive model (Karimi *et al.*, 2014; Gao *et al.*, 2009):

$$W = a_{10}(I_1 - 3) + a_{01}(I_2 - 3) + a_{20}(I_1 - 3)^2 + a_{11}(I_1 - 3)(I_2 - 3) + a_{02}(I_2 - 3)^2 + \frac{1}{d}(J - 1)^2 \quad (2)$$

$I_1$  and  $I_2$  are the first and second strain invariants;  $a_{10}$  ( $-4.020 \text{ MPa}$ ),  $a_{01}$  ( $4.321 \text{ MPa}$ ),  $a_{20}$  ( $18.401 \text{ MPa}$ ),  $a_{11}$  ( $-51.856 \text{ MPa}$ ) and  $a_{02}$  ( $39.105 \text{ MPa}$ ) are the hyperelastic constants describing the deformation;  $d$  is the incompressible parameter ( $2.434 \text{ MPa}^{-1}$ ); and  $J$  is the

elastic volume ration. The arterial wall density,  $\rho_w$ , was considered constant and equal to 1120 kg/m<sup>3</sup> (Gao *et al.*, 2009).

### BOUNDARY CONDITIONS

A physiological velocity and pressure transient profiles assembled using Fourier series were implemented in the model (Figure 2). At the inlet, the transient Womersley velocity profile which is time-dependent and radius-dependent was imposed (Pinto *et al.*, 2018):

$$v(r, t) = \frac{AR^2}{i\mu\alpha^2} \left( 1 - \frac{J_0(i^{3/2}\alpha\frac{r}{R})}{J_0(i^{3/2}\alpha)} \right) e^{i\omega t} \quad (3)$$

The pressure waveform considered in all the system outlets is also time-dependent (Figure 2). For a healthy individual, the pressure at systolic peak (maximum velocity) is around 120 mmHg while the pressure at the diastole ( $p_{diastole}$ ) is 80 mmHg (Figure 2). Since the CT images were captured at diastolic phase, the temporal pressure gradient applied,  $P(t)$ , was set (Torii *et al.*, 2009, Park *et al.*, 2011) in order to maintain the vessels pressurized:

$$P(t) = p(t) - p_{diastole} \quad (4)$$

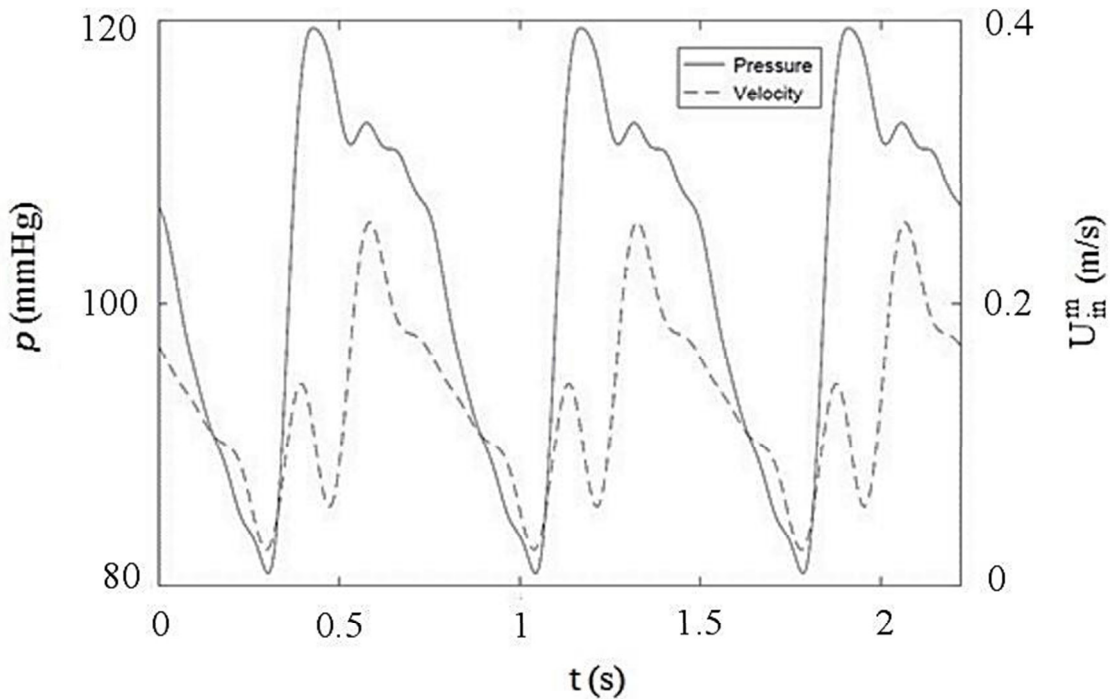


Fig. 2 - Mean transient velocity profile,  $U_{in}^m$ , at the inlet, and pressure waveform,  $p$ , at the outlet sections.

Furthermore, all the degrees of freedom from all the nodes in the inlet and the outlets faces were constrained.

## FLUID-STRUCTURE INTERACTION METHOD

The simulations, performed in ANSYS® software (Ansys Inc., Swanson, Canonsburg, USA) and in the In-House OpenFOAM® software, were result of the interaction between the CFD and the structural model, solved independently.

For ANSYS® simulations, SIMPLE algorithm was used, in the CFD model, to solve the velocity-pressure coupled equations; and QUICK and PRESTO schemes were used, respectively, to discretize the momentum and pressure term (Park *et al.*, 2011). Once the fluid domain has been solved and converged, the calculated pressure gradient is transferred to the fluid-structure interface, where the structural domain calculates the resulting displacements. After the converged solution, the fluid mesh is updated through a diffusion-based smoothing method.

The In-House OpenFOAM code is an open-source written in C++ and uses an object oriented approach which makes it easy to extend. The numerics implemented in the In-House OpenFoam uses the Finite Volume Method on unstructured meshes.

## RESULTS AND CONCLUSIONS

The overlap of the In-House OpenFOAM profile with the Ansys® profile, using FSI method, shows the accuracy and validation of the results (Figure 3b). The velocity magnitude, at systolic peak, was achieved in several locations (Figure 3a) in order to better understand the differences and the importance of the arterial wall deformation (FSI) comparatively to the rigid model (CFD).

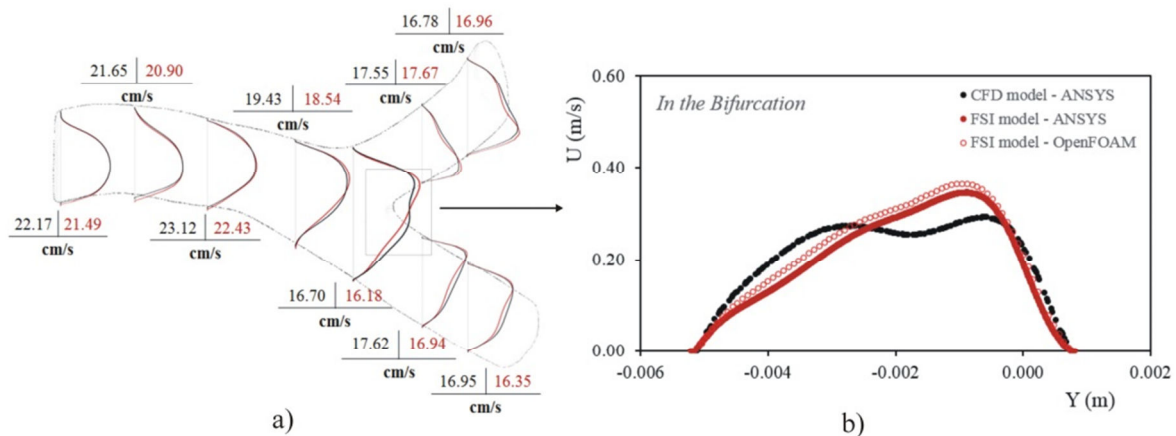


Fig. 3 - Comparison between the velocity profiles and the mean velocity using CFD and FSI models. (a) in several locations; (b) in the bifurcation detail.

Near the inlet and outlets, the contours are identical due to the fixed constrain applied (Figure 3a). However, in the bifurcation, the profiles differ significantly (Figure 3). The dynamic

behavior results in a global reduction of 3.5% due to the increase of the fluid domain during the pulsatile flow: higher sectional area leads to a smaller mean velocity.

## **ACKNOWLEDGMENTS**

The authors gratefully acknowledge the Foundation for Science and Technology Portugal (FCT), the Research Unit of LAETA-INEGI, Engineering Faculty of University of Porto, and the Cardiovascular R&D Unit of the Medicine Faculty of University of Porto.

## **REFERENCES**

- [1] Chaichana T, Sun Z, Jewkes J. Hemodynamic impacts of various types of stenosis in the left coronary artery bifurcation: A patient-specific analysis. *Physica Medica*, 2013, 29, pp. 447-452.
  
- [2] Gao H, Long Q, Graves M, Gillard JH, Li ZY. Carotid arterial plaque stress analysis using fluid-structure interactive simulation based on in-vivo magnetic resonance images of four patients. *J Biomech*, 2009, 42, pp. 1416-1423.
  
- [3] Guerciotti B, Vergara C, Ippolito S, Quarteroni A, Antona C, Scrofani R. A computational fluid-structure interaction analysis of coronary Y-grafts. *Med. Eng. Phys.*, 2017, 47, pp. 117-127.
  
- [4] Mozaffarian D, Benjamin EJ, Go AS et al. Heart disease and stroke statistics. *Circulation*, 2015, 131, pp. e29-322.
  
- [5] Park C.G. and Lee J.Y. The Significance of the J-Curve in Hypertension and Coronary Artery Diseases, *Korean Circ. J.*, 2011, 41, pp. 349-353.
  
- [6] Pinto SIS, Campos JBLM, Azevedo E, Castro CF, Sousa LC. Numerical study on the hemodynamics of patient-specific carotid bifurcation using a new mesh approach. *Int J Numer Meth Biomed Engng*. 2018; e2972.
  
- [7] Torii R, et al. Fluid-structure interaction analysis of a patient-specific right coronary artery with physiological velocity and pressure waveforms. *Commun. Numer. Methods Eng.*, 2009, 25, pp. 565-580.
  
- [8] van der Giessen AG, Groen HC, Doriot P-A, Feyter PJ, van der Steen AFW, van de Vosse FN, Wentzel JJ, Gijzen FJH. The influence of boundary conditions on wall shear stress distribution in patients specific coronary trees. *Journal of Biomechanics*, 2011, 44, pp. 1089-1095.

[9] Xie X, Wang Y, Zhu H, Zhou J. Computation of hemodynamics in tortuous left coronary artery: a morphological parametric study. *J Biomech Eng*, 2014, 136, pp. 101006-1-9.

[10] Zhang Q, Gao B, Chang Y. Effect of Different Rotational Directions of BJUT-II VAD on Aortic Swirling Flow Characteristics: A Primary Computational Fluid Dynamics Study. *Med Sci Monit*, 2016, 22, pp. 2576-2588.